Influence of Partial Metal Ion Substitution on the Temperature Evolution of the Optical Absorption Edge in $((CH_3)_2CHNH_3)_4Cd_3Cl_{10}$:Cu Crystals

V. Kapustianyk[a,b], P. Yonak[b,*], V. Rudyk[a], Z. Czapla[c,d] and R. Cach[d]

[a]Scientific-Technical and Educational Center of Low-Temperature Studies, Ivan Franko National University of Lviv, Dragomanova Str. 50, 79005 Lviv, Ukraine

[b]Department of Physics, Ivan Franko National University of Lviv, Dragomanova Str. 50, 79005 Lviv, Ukraine

[c]Department of Physics, Opole University of Technology, Ozimska 75, 45-370 Opole, Poland

[d]Institute of Experimental Physics, University of Wrocław, Pl. M. Borna 9, 50204 Wrocław, Poland

On the basis of absorption spectroscopy data the temperature evolution of the optical absorption edge in the region of phase transitions of $[(CH_3)_2CHNH_3]_4Cd_3Cl_{10}$ (IPACC) and the same crystal doped with Cu^{2+} (IPACCC) was studied. Performed investigations ascertained a noticeable influence of the doping with Cu^{2+} ions on the exciton–phonon interaction and respectively on the shape and temperature evolution of the optical absorption edge of IPACC crystals. It has been found that characteristic parameters of Urbach's rule show anomalous behaviour at the phase transition point $T_2 = 293$ K. It was shown that the low energy tail of the charge transfer band in IPACCC is formed with participation of the internal vibrations of the metal–halogen complex. On the other hand, the low energy tail of the fundamental edge for both IPACC and IPACCC is formed with participation of the internal vibrations of the metal–halogen complex or skeletal (or translational) vibration of IPA cation.

1. Introduction

Unusual structural architectures are formed in halogeno-cadmate (II) compounds. Owing to the chemical flexibility of these hybrid organic-inorganic materials, it is possible to create different crystal structures in order to optimize their physical properties [1, 2]. Cadmium compounds are also interesting from the point of view of the role of this metal in the biological processes [3].

Various anionic substructures may be generated in types of materials such as isolated octahedral and tetrahedral units, one-dimensional linear chains, ribbon-like structures, and two-dimensional layers, by sharing triangular faces, edges, or vertices of octahedra. A wide variety of stoichiometries have been found in this class of material, e.g. $CdCl_3$ [4], Cd_3Cl_9 [5], $CdCl_4$, Cd_3Cl_{10} [6], $CdCl_6$ [7], Cd_3Cl_{11} [8], $[C_6H_{10}N_2]_2Cd_3Cl_{10}$, and $[C_4H_{14}N_2]Cd_3Cl_{10}$ which possess an interesting structure where the anionic substructure consists of one-dimensional polymeric $(Cd_3Cl_{10})_n^{4n-}$ chains [9]. $[C_6H_8N]^{4+}[Cd_3Cl_{10}]^{4-}$, on the other hand, crystallizes with a two-dimensional layered network of $(Cd_3Cl_{10})^{4-}$ linear trimers that are interconnected by bridging corner-shared chlorides [1].

IPACC exhibits several temperature-dependent phase transitions and the structures of the individual phases

were studied. Dielectric, dilatometric, X-ray, differential scanning calorimetry (DSC), and optical studies [10–12] showed and confirmed three phase transitions at temperatures $T_1 = 353$ K, $T_2 = 294$ K, and $T_3 = 260$ K [10].

The crystal structure of IPACC consists of two-dimensional network of Cd_3Cl_{10} units interconnected by isopropylammonium cations. According to the data of [10] face-sharing $CdCl_6$ octahedra form a $[Cd_3Cl_{10}]_4$ polyanion. In the high temperature phase I the $CdCl_6$ octahedra are distorted. The octahedron I around Cd2 in $2/m$ is tetragonally compressed as the two axial Cd2–Cl4 bonds are shorter by 0.066 Å than those in the equatorial plane. The initial molecular symmetry of such an octahedron would be D_{4h}. In the m symmetry there are two similar octahedra (further — octahedron II) with the Cd1(Cd3)–Cl6 distances ranging from 2.4839 (5) to 2.7126 (3) Å. Although the one pair of distances is considerably larger than other four, this octahedron possesses the symmetry lower than tetragonal. At the phase transitions to the low temperature phases both types of octahedra become more distorted [10].
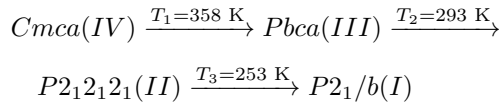
As it was suggested in [13], new IPACCC compounds due to doping with Cu^{2+} ions has generated special interests for scientists, since they could reveal principally new magnetic properties and possible magnetoelectric coupling. Indeed, the related crystals with an alkylammonium cation and transition metal ions in their structure were found to be multiferroics since they are characterised by coexistence of ferroelectric and magnetic ordering [14–16]. Besides, it has been shown that the

---

*corresponding author; e-mail: yonak.pavlo@gmail.com

partial isomorphous substitution of Al^{3+} ion with transition metal Cr^{3+} is followed by a drastic change of magnetic and electric properties in the paramagnetic ferroelectric $NH_2(CH_3)_2Al_{1-x}Cr_x(SO_4)_2 \cdot 6H_2O$ in comparison with an initial diamagnetic crystal with $x = 0$. Moreover, it was demonstrated that varying the rate of substitution ($x = 0.065$, $x = 0.20$) one can induce and even tune the sign of the magnetoelectric interactions that were found to be among the largest in the family of the known multiferroics [17]. Therefore, one can conclude that the effective interaction between magnetic moments and electric charges, which is considered as an important phenomenon in the modern solid state physics and spin electronics, would be realised in the organometallic compounds by means of isomorphous substitution with transition metal ion [17].

On the other hand, the compounds of such a type could be also interesting for nonlinear optics applications [18–20]. Doping of these crystals with transition metal ions implies possibility of the quite large photoinduced effects, for example, second harmonic generation.

For the first time the properties of IPACCC crystals were reported in [13]. The energy dispersive X-ray (EDX) analysis showed that the amount of Cu doping is about 0.5%. It was suggested that the sequence of phases and their structures in IPACCC is very similar to those in the initial crystals and some Cd atoms are statistically replaced by Cu atoms in anionic complex $[Cd_3Cl_{10}]^{4-}$. This conclusion is confirmed by the data of X-ray diffraction, heat capacity and crystal field spectra study of IPACCC crystals [21]. Besides it was shown that the temperatures of corresponding phase transitions in the doped crystals are a little shifted with respect to the initial one

$$Cmca(IV) \xrightarrow{T_1=358 \text{ K}} Pbca(III) \xrightarrow{T_2=293 \text{ K}}$$

$$P2_12_12_1(II) \xrightarrow{T_3=253 \text{ K}} P2_1/b(I)$$

This paper is devoted to comparative study of temperature evolution of the optical absorption edge in the region of phase transitions of IPACC and IPACCC crystals. The main purpose consists of analysis of nature of the electron– (exciton–)phonon interaction (furthermore — EPI) and corresponding parameters in different phases of the investigated ferroics.

2. Experimental

IPACC and IPACCC crystals were grown at $T = 304$ K from an aqueous solution of $CdCl_2 \cdot 4\ H_2O$ and $(CH_3)_2NH_2Cl$ salts taken in the stoichiometric ratio with a small excess of HCl. In the case of IPACCC, corresponding amount of $CuCl_2$ was added into the solution.

The absorption spectra were measured using automated site based on ZMR-3 monochromator at the thin ($0.5 \div 3$ mm) freshly cleaved crystalline platelets (parallel to the layers). The polarized and nonpolarized light was propagated along the principal axes of the crystal.

A special liquid helium cryostat together with a temperature controller "UTREX" and the germanium temperature sensor provided necessary precision of the temperature measurements and stabilization ($\Delta T = \pm 0.1$ K).

3. Results and discussion

The polarized absorption spectra of IPACCC crystals are shown in Fig. 1 in comparison with those for initial IPACC. The absorption bands observed within the range of $650 \div 1050$ nm are characteristic of the internal transitions of the Cu^{2+} ion being in the distorted octahedral co-ordination of the chlorine ions. Details of the temperature evolution of the crystal field absorption spectra are described in [13]. The intensive absorption peaks observed at the energies higher than 2.9 eV (250–450 nm) are attributed to the charge transfer (CT) transition Cl $3p \rightarrow$Cu $3d$. Their low energy tail forms the additional absorption edge in IPACCC (see Fig. 2). At the higher energies ($\lambda < 250$ nm) for both crystals one can observe the optical absorption edge that would be related to the electron transitions of Cl $3p \rightarrow$Cd $5s$ type (transition from the top of valence band on the bottom of conductivity band) which will be analyzed furthermore.
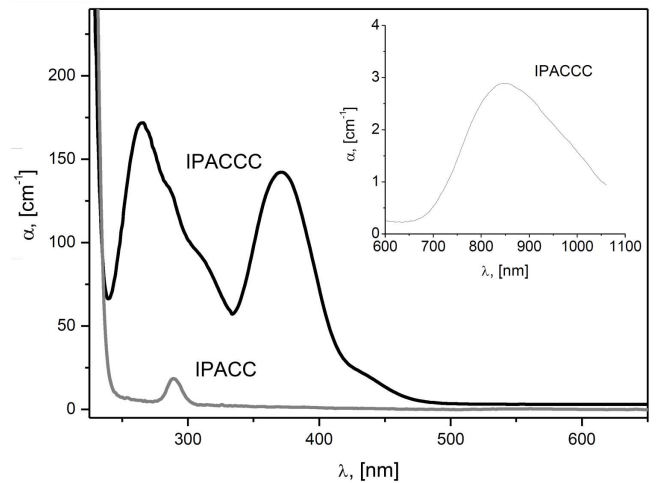

Fig. 1. The comparison of the absorption spectra of IPACC and IPACCC, at room temperature obtained for light polarisation $E||a$.

As it follows from Fig. 2, the high energy absorption edge does not show any pronounced pleochroism, whereas the position and, most of all, the intensities of the CT bands considerably depend on polarization of light reflecting the distortion of the Cu^{2+} ion coordination.

Due to presence of Cu^{2+} in their crystalline structure IPACCC type crystals become appropriate substances for investigations of electron– (exciton–)phonon interaction (furthermore — EPI). Study of temperature evolution of
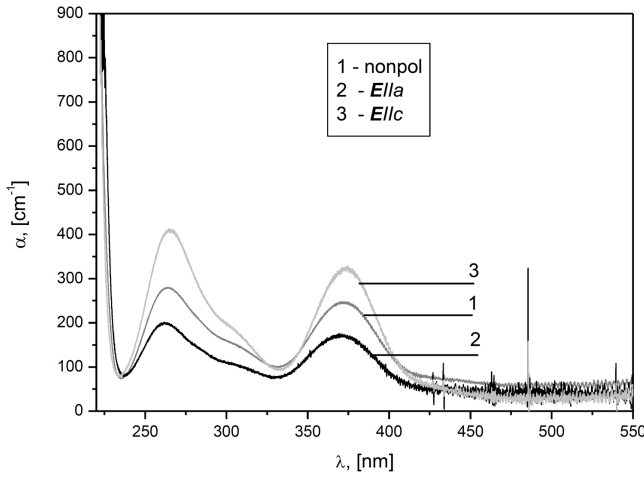
Fig. 2. The absorption spectra of IPACCC, at room temperature obtained for light polarisations $E||a$, $E||c$ and for nonpolarized light.

the absorption edge in the aforementioned crystals should be considered as a very interesting scientific problem. It remains important for the physics of solid state, first of all, due to the variety of attempts to explain the appearance of low energy tail of the edge band in different crystals. The temperature evolution of the optical absorption edge in A_2BX_4 type compounds with an alkylammonium cation was analyzed in detail in [22]. It has been shown that for most phases of these crystals with exception of the incommensurate ones the absorption edge follows the empirical Urbach rule:

$$\alpha = \alpha_0 \exp\left(\frac{\sigma(T)}{k_B T}(\hbar\omega - E_0)\right), \qquad (1)$$

where α_0, E_0 are the constants, $\hbar\omega$ is the energy of photons, and k_B is the Boltzmann constant. The parameter $\sigma(T)$ characterizes the broadening of the absorption edge.

It is almost evident that for the A_2BX_4 and ABX_3 type compounds with an alkylammonium cation this exponential tail originates in the electron– or exciton–phonon interaction discussed by a number of authors. In this case $\sigma(T)$ parameter, usually, is presented as

$$\sigma(T) = \sigma_0 \frac{2k_B T}{\hbar\omega_0} \tanh\left(\frac{\hbar\omega_0}{2k_B T}\right), \qquad (2)$$

where the dimensionless σ_0 parameter is connected with the constant of EPI, $\hbar\omega_0$ is the effective energy of phonons interacting with photons.

Some characteristic features of the EPI in the A_2BX_4 type compounds with an alkylammonium cation have been ascertained in [22] with employment of the Sumi–Toyozawa model [23]. In particular, it was shown that the strength of EPI, which is inversely proportional to the parameter σ_0, considerably depends on the nature of the edge band. A small value of σ_0 in the H-bonded compounds was associated with presence of the exciton absorption band composed of the alkylammonium heads. In this case the comparatively strong exciton–phonon in-

teraction is fairly well described by the model of the self-trapped exciton. On the other hand, when the low energy tail is formed by the transitions of CT Cl $3p \rightarrow$Me $3d$ or transitions of Cl $3p \rightarrow$Me $4s$ (Me $5s$) type, the strength of EPI was found to be much lower. These conclusions should be simply checked by comparison of IPACC and IPACCC since these crystals manifest the intensive bands of the mentioned types within the appropriate spectral region. Under such circumstances comparing the data concerning the temperature evolution of the absorption edge in IPACC and IPACCC crystals one could obtain the information about the difference in the nature of EPI in both cases.

In the case of initial IPACC crystal one can conclude that the optical absorption edge is not formed with participation of the self-trapped exciton contrary to the case of other compounds with alkylammonium cations, that are characterised by much more pronounced broadening of the edge [22, 23]. Under such circumstances the edge band for both investigated crystal are thought to arise at the energies higher than 5.15 eV due to Cl $3p \rightarrow$Cd $5s$ transitions involving participation of free excitons. The low energy tail of this band forms the absorption edge both in IPACC and IPACCC. Such a conclusion is confirmed by the detailed analysis of the parameters empirical Urbach rule.

Figure 3 and 4 present temperature evolution of the low energy tails of the fundamental edge band for IPACC and for IPACCC and charge transfer bands for IPACCC. Corresponding dependences of the absorption coefficient in the logarithmic scale on energy are presented for different temperatures within the two different phases — II and III. We limited our investigations to the temperature range between T_1 and T_3 — temperatures of the first order phase transition. Below T_3 a sample is usually cracked due to arising mechanical tensions and cannot be used anymore for further optical investigations. In order to avoid the influence of the similar tensions and corresponding cracks on the experimental results also around T_1 we do not perform the investigations above this temperature.

According to (1) $\ln\alpha = f(E)$ dependences in the vicinity of low energy tail of the fundamental absorption edge possess a straight-line character and cross at one point with the coordinates E_0 and α_0 (see Table I) for majority of phases and polarizations for both investigated crystals (Fig. 3). Availability of a single crossing point testifies to the fulfilment of the Urbach rule. On the other hand, in the case of the high temperature phase II in IPACCC for polarization $E||a$ (Fig. 3c) $\ln\alpha = f(E)$ lines do not cross at a single crossing point. Such behaviour can be explained by overlapping of the mentioned absorption edge with the neighbouring CT bands.

One can also note that the low energy tail of the CT bands in IPACCC also follows the Urbach rule (Fig. 4) although the corresponding crossing point is shifted considerably towards lower energies with respect to the case of the fundamental edge (Fig. 3).
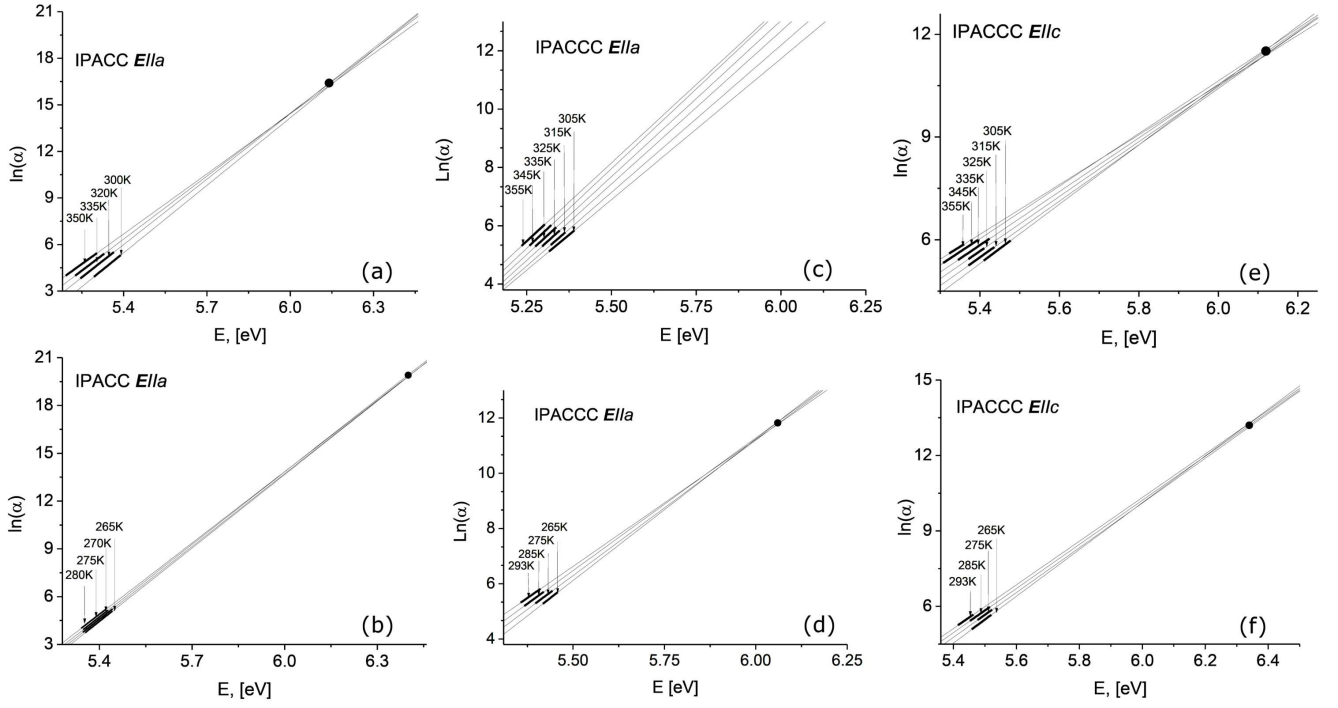
Fig. 3. Dependences of $\ln \alpha$ on the photon energy in vicinity of the fundamental absorption edge, obtained at different polarizations of light for the high temperature ($T > T_2$) (a, c, e) and the low temperature phases ($T < T_2$) (b, d, f) of IPACC and IPACCC crystals.
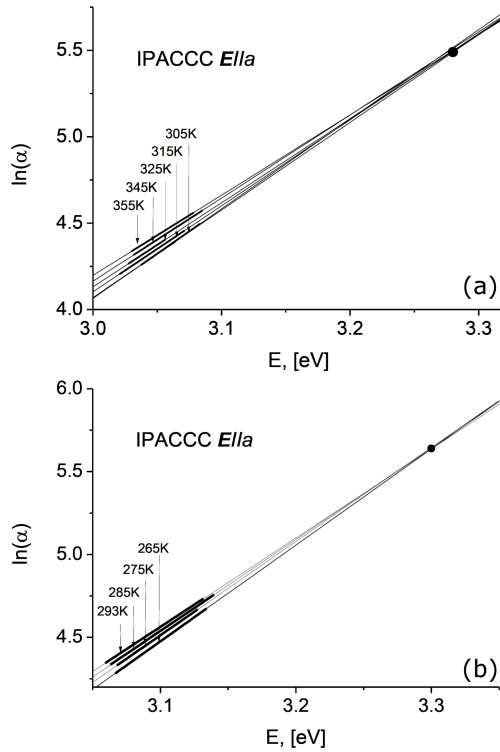

Fig. 4. Dependences of $\ln \alpha$ on the photon energy in vicinity of the low energy tail of the CT band of IPACCC for polarization of light $E || a$ and different temperatures within: (a) high temperature phase II ($T > T_2$), (b) low temperature phase III ($T < T_2$).

TABLE I

Urbach's parameters of IPACCC and IPACC (fund. — fundamental)

	Temp. [K]	$\ln \alpha_0$	E_0 [eV]	$\tilde{\nu}_0$ [cm^{-1}]	σ_0	Identification of phonons
IPACC	255–294	19.9	6.4	485	0.535	C–C–N
(fund.) $E||a$	294–353	16.4	6.14	155	0.394	ν_2 Me–Cl
IPACCC	255–293	11.9	6.06	157	0.247	ν_2 Me–Cl
(fund.) $E||a$	293–355	–	–	–	–	
IPACCC	255–293	13.2	6.34	335	0.266	ν_3 Me–Cl
(fund.) $E||c$	293–355	11.51	6.12	75	0.228	trans C–C–N
IPACCC	255–295	5.64	3.3	267	0.155	ν_1 Cu–Cl
(CT) $E||a$	293–355	5.49	3.28	338	0.164	ν_3 Cu–Cl

Analyzing the obtained data, it is necessary to note that Figs. 3 and 4 present the dependences and corresponding extrapolating lines in the very wide scale of energies and the absorption coefficients in order to demonstrate the intersection point. Under such circumstances there appears an impression of lack of data to be processed. In fact, for each extrapolation case we have used several tens of data points. The corresponding experimental data in the more appropriate coordinates and scales are presented in Figs. 1 and 2.

The steepness of the aforementioned linear dependences determines the parameter σ for a certain temperature

$$\sigma(T) = \frac{\Delta(\ln k)}{\Delta(\hbar\omega)} k_{\mathrm{B}} T. \qquad (3)$$

Its temperature dependence as well as the isoabsorption temperature dependence of the energy E' corresponding to a constant value of α (Fig. 5) would be sensitive to the phase transitions. In spite of some subjectivity in the determination of E', this parameter, at least, reflects the energy position of the absorption edge. As it is clearly seen from Fig. 6, this parameter for the fundamental edge shows only a very weak change of slope in vicinity of $T_2 = 293$ K for IPACCC. Such a behaviour testifies that character of EPI in this case is not affected noticeably by the phase transition in both compared crystals. On the other hand, corresponding parameter for the edge of the CT band in IPACCC manifests a clear change of slope at the mentioned phase transition reflecting a more considerable change of the EPI. As it is clearly seen from Fig. 6, the corresponding $\sigma(T)$ dependences manifests much more pronounced anomalies at the phase transition point T_2 for IPACCC than in the case of the initial crystal. One can conclude that the EPI is more affected by this phase transition in the crystal doped with copper. More detailed information concerning these changes would be drawn from the analysis of the parameters of the empirical Urbach rule (1).

Fig. 6. As in Fig. 5, but for the parameter $\sigma(T)$.
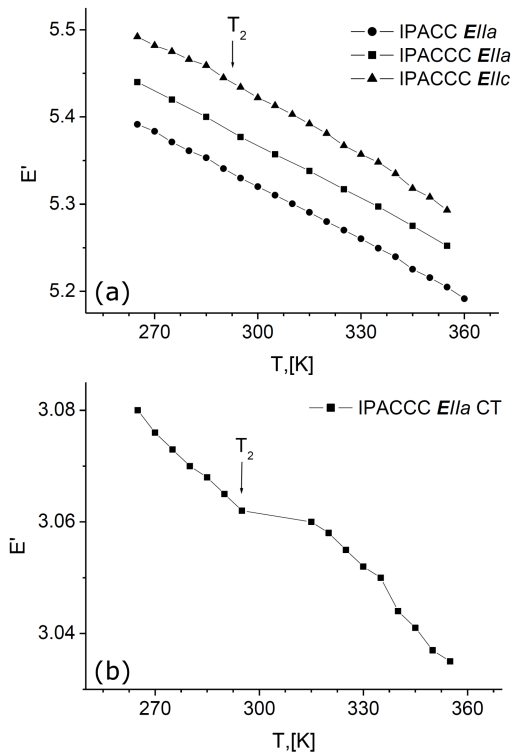

Fig. 5. Temperature dependences of the parameter $E'(T)$ for the fundamental edge (a) and charge transfer (b) band.

Every phase of IPACCC, in principle, possesses its own σ_0 and $\hbar\omega_0$ constants in the case of fulfilment of the Urbach rule. These parameters are calculated on the basis of Eq. (2). In Table I the data obtained are compared for both investigated crystals.
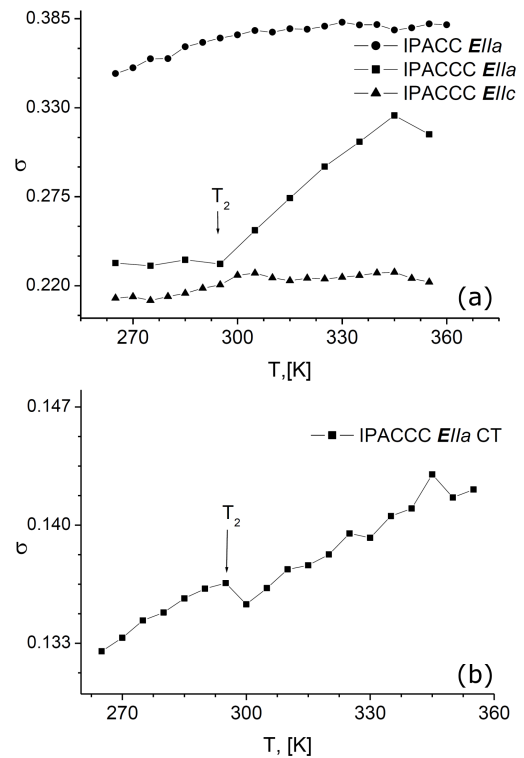
The values of effective energy $\hbar\omega_0$ calculated for different phases of both crystals would be more convenient to present as the wave numbers. In such a case it would be easy to compare them with certain vibration modes obtained by means of vibrational spectroscopy [24]. These effective values of the phonons participating in the EPI were found to be very close to the energies (wave numbers) of the real internal vibration of the metal–halogen octahedra and skeletal (or translational) vibration of IPA cation. It has been found that the low energy tail of the CT band in the phases II and III of IPACCC is formed with participation of the internal vibrations of the metal–halogen complex. This looks natural since the process of charge transfer proceeds exactly within this complex. Concerning the tail of the fundamental edge for IPACCC, it is formed with participation of the internal vibrations of the metal–halogen complex in the phase III and translational vibration of IPA cation in the phase II ($E\|c$). On the other hand, the skeletal vibrations of the organic group (C–C–N) are mostly responsible for the formation of the absorption edge in the low temperature phase II, whereas the internal vibrations of the metal–halogen complex participate in this process in the high temperature phase of IPACC.

In spite of the fact that the values of effective phonon energies generally were found to be close for both compared crystals, a considerable difference was observed in the values of σ_0. Concerning the low energy tail of the fundamental edge, one can note a considerably larger value of the mentioned parameter for both phases in the

initial crystal that implies much smaller value of the EPI strength and respectively less pronounced broadening of the edge than in IPACCC. The second conclusion for the copper doped crystal would be that the CT band is characterised by smaller values of σ_0 compared to those for the fundamental edge. This reflects in a more pronounced broadening due to EPI.

4. Conclusion

Performed spectral investigations ascertained a noticeable influence of the doping with Cu^{2+} ions on the exciton–phonon interaction and respectively on the shape and temperature evolution of the optical absorption edge of IPACC crystals. Due to this interaction, for the phases II and III of both IPACC and IPACCC crystals, the low energy tails of the edge bands are described by the empirical Urbach rule. The only exception concerns the phase II in IPACCC for the light polarised along a axis, when $\ln \alpha = f(E)$ lines were found to not cross at a single point. Such a behaviour is explained by overlapping of the mentioned absorption edge with the CT bands. It has been found that characteristic parameters of the Urbach rule show anomalous behaviour at the phase transition point T_2. It is important to note that the corresponding $\sigma(T)$ and $E'(T)$ dependences manifest much more pronounced anomalies at the phase transition point T_2 for IPACCC than in the case of the initial crystal that implies more considerable corresponding change of EPI character for the crystals doped with copper.

It has also been found that the low energy tail of the CT band in IPACCC is formed due to participation of the internal vibrations of the metal–halogen complex that is connected directly with the charge transfer proceeding exactly within this complex. On the other hand, the low energy tail of the fundamental edge for both IPACC and IPACCC is formed due to participation of the internal vibrations of the metal–halogen complex or skeletal (or translational) vibration of IPA cation.

It was also shown that partial metal ion substitution is followed by increase in of the EPI strength in the investigated crystals. Taking into account the calculated values of σ_0 constant according to the classification proposed in [22] the fundamental edge band for both investigated crystal would be related to Cl $3p \rightarrow$ Cd $5s$ transitions. Their low energy tail similarly to those for the CT band would be described on the basis of the Sumi–Toyozawa model involving participation of free excitons.

References

[1] Ch.E. Costin-Hogan, C.L. Chen, E. Hughes, A. Pickett, R. Valencia, N.P. Rath, A.M. Beatty, *Cryst. Eng. Commun.* **10**, 1910 (2008).

[2] A. Thorn, R.D. Willett, B. Twamley, *Cryst. Growth Des.* **5**, 673 (2005).

[3] L.G. Marzilli, T.J. Kistenmacher, G.L. Eichhorn, in: *Metal Ions in Biology*, Ed. T.G. Spiro, Wiley, New York 1980, p. 179.

[4] I. Peral, G. Madariaga, A. Pérez-Etxebarria, T. Breczewski, *Acta Crystallogr. B* **56**, 215 (2000).

[5] F.F. Jian, P.S. Zhao, Q.X. Wang, Y. Li, *Inorg. Chim. Acta* **359**, 1473 (2006).

[6] I. Chaabane, F. Hlel, K. Guidara, *PMC Phys. B* **1**, 11(2008).

[7] S. Sakida, H. Nakata, Y. Kawamoto, *Solid State Commun.* **127**, 447 (2003).

[8] A. Waśkowska, T. Lis, U. Krzewska, Z. Czapla, *Acta Crystallogr. C* **46**, 1768 (1990).

[9] A.B. Corradi, S. Bruckner, M.R. Cramarossa, T. Manfredini, L. Menabue, M. Saladini, A. Saccani, F. Sandrolini, J. Giusti, *Chem. Mater.* **5**, 90 (1993).

[10] A. Gagor, A. Waśkowska, Z. Czapla, S. Dacko, *Acta Crystallogr. B* **67**, 122 (2011).

[11] B. Staśkiewicz, S. Dacko, Z. Czapla, *Curr. Appl. Phys.* **12**, 413 (2012).

[12] J. Przesławski, M. Kos, Z. Czapla, *Thermochim. Acta* **546**, 49 (2012).

[13] V. Kapustianyk, P. Yonak, V. Rudyk, Z. Czapla, D. Podsiadła, Y. Eliyashevskyy, A. Kozdraś, P. Demchenko, R. Serkiz, *J. Phys. Chem. Solids* **121**, 210 (2018).

[14] B. Kundys, A. Lappas, M. Viret, V. Kapustianyk, V. Rudyk, S. Semak, C. Simon, I. Bakaimi, *Phys. Rev. B* **81**, 224434 (2010).

[15] V. Kapustianyk, V. Rudyk, P. Yonak, B. Kundys, *Phys. Status Solidi B* **252**, 1778 (2015).

[16] Y. Tian, A. Stroppa, Y. Chai, L. Yan, S. Wang, P. Barone, S. Picozzi, Y. Sun, *Sci. Rep.* **4**, 6062 (2014).

[17] V. Kapustianyk, Y. Eliyashevskyy, Z. Czapla, V. Rudyk, R. Serkiz, N. Ostapenko, I. Hirnyk, J.-F. Dayen, M. Bobnar, R. Gumeniuk, B. Kundys, *Sci. Rep.* **7**, 14109 (2017).

[18] B. Sahraoui, R. Czaplicki, A. Klöpperpieper, A.S. Andrushchak, A.V. Kityk, *J. Appl. Phys.* **107**, 113526 (2010).

[19] W. Bi, N. Louvain, N. Mercier, J. Luc, I. Rau, F. Kajzar, B. Sahraoui, *Adv. Mater.* **20**, 1013 (2008).

[20] N. Mercier, A. Barres, M. Giffard, I. Rau, F. Kajzar, B. Sahraoui, *Angew. Chem. Int. Ed.* **45**, 2100 (2006).

[21] B. Staśkiewicz, J. Baran, Z. Czapla, *J. Phys. Chem. Solids* **74**, 1848 (2013).

[22] V. Kapustianyk, *Phys. Status Solidi B* **204**, 877 (1997).

[23] H. Sumi, A. Sumi, *J. Phys. Soc. Jpn.* **56**, 2211 (1987).

[24] V. Kapustianik, *Phys. Status Solidi B* **207**, 509 (1998).